Proceedings of the ASME 2014 Dynamic Systems and Control Conference
DSCC 2014
October 22-24, 2014, San Antonio, TX, USA

DESIGN AND DYNAMIC MODELING OF A FLEXIBLE FEATHERING JOINT FOR ROBOTIC FISH PECTORAL FINS

Sanaz Bazaz Behbahani *†
Smart Microsystems Laboratory
Department of Electrical and Computer Engineering
Michigan State University
East Lansing, Michigan 48824
Email: bazazbeh@egr.msu.edu

Xiaobo Tan
Smart Microsystems Laboratory
Department of Electrical and Computer Engineering
Michigan State University
East Lansing, Michigan 48824
Email: xbtan@egr.msu.edu

ABSTRACT

In this paper, we propose a novel design for a pectoral fin joint of a robotic fish. This joint uses a flexible part to enable the rowing pectoral fin to feather passively and thus reduce the hydrodynamic drag in the recovery stroke. On the other hand, a mechanical stopper allows the fin to maintain its motion prescribed by the servomotor in the power stroke. The design results in net thrust even when the fin is actuated symmetrically for the power and recovery strokes. A dynamic model for this joint and for a pectoral fin-actuated robotic fish involving such joints is presented. The pectoral fin is modeled as a rigid plate connected to the servo arm through a pair of torsional spring and damper that describes the flexible joint. The hydrodynamic force on the fin is evaluated with blade element theory, where all three components of the force are considered due to the feathering degree of freedom of the fin. Experimental results on robotic fish prototype are provided to support the effectiveness of the design and the presented dynamic model. We utilize three different joints (with different sizes and different flexible materials), produced with a multi-material 3D printer, and measure the feathering angles of the joints and the forward swimming velocities of the robotic fish. Good match between the model predictions and experimental data is achieved, and the advantage of the proposed flexible joint over a rigid joint, where the power and recovery strokes have to be actuated at different speeds to produce thrust, is demonstrated.

INTRODUCTION

Bio-inspired robotic systems have received significant attention over the past several decades [1]. An important branch of bio-inspired robotics is dedicated to fish-like aquatic robots [2–5]. High maneuverability and efficiency of fish swimming have motivated the development of a number of robotic fish prototypes [6–10]. Besides mimicking live fish swimming behavior [5, 7], a bio-inspired robotic fish can perform different tasks, from monitoring aquatic environments [11–13], to interacting with live fish to study their social behavior [14].

Propulsion mechanisms of robotic fish have included oscillatory caudal fin [8, 15–17], paired pectoral fins [18–21], or a combination of both tail and pectoral fins [6]. While actuation with paired pectoral fins have received less attention compared to caudal fin actuation, the pectoral fins play an important role in agility and maneuverability of fish swimming [22]. Earlier studies on live fish pectoral fins were performed by Webb [23] and Blake [24] in late 70's and early 80's. Their methods for the calculation of hydrodynamic forces on pectoral fins are still used today to study pectoral fin behavior. Work on pectoral fin-actuated robotic fish has mainly involved rigid, oscillatory pectoral fins [6, 25–28]. Some limited work has been reported on flexible pectoral fins, which typically uses Computational Fluid Dynamics (CFD)-based modeling [29]. In our prior work we presented a dynamic model for flexible pectoral fins with rigid joints [18], and proposed the design of a passive, *rowing* joint for the pectoral fins [30]. In both cases, the fin is restricted to the rowing motion only, where the hydrodynamic force is considered to be limited to the 2D horizontal plane.

*Address all correspondence to this author.

†This work was supported by National Science Foundation (Grant DBI-0939454, CNS-1059373, IIS-0916720 , IIS-1319602, and CCF-1331852).

To more precisely mimic live fish pectoral fin motion, the fins need to have more degrees of freedom, such as feathering or flapping motion. To be able to do so without adding another source of actuation to the robot, the authors present in this paper a novel design of a passively rotating (feathering) flexible joint for the pectoral fins. The joint is used to connect the pectoral fin to the actuation mechanism (servo arm), which generates the rowing motion. This design, with the help of a mechanical stopper, allows the pectoral fin to feather during the recovery stroke thus reducing the hydrodynamic drag, while maintaining the prescribed rowing motion in the power stroke, which generates good amount of net thrust during each cycle.

The remainder of the paper is organized as follows. First, the design and prototyping of the feathering passive joint is described in detail. Next, the modeling of the joint as well as that of the robotic fish adopting pectoral fins with such joints are discussed. The hydrodynamic forces on the pectoral fins are calculated with blade element theory, where the forces during the power stroke are considered to remain in the horizontal plane, while those during the recovery stroke involve all three components. The flexible joint is modeled as a pair of torsional spring and damper. Experimental results on a robotic fish prototype are then provided to validate the dynamic model. Joints with different sizes and stiffnesses are used, along with comparison with a rigid joint. The experimental results support the effectiveness of the proposed design in producing thrust with symmetric actuation in power and recovery strokes, demonstrate its advantage over the traditional rigid fin joint, and validate the proposed model for the passive feathering joint and the robotic fish. Finally, concluding remarks and brief discussion on future work are presented.

DESIGN AND PROTOTYPING OF THE FLEXIBLE FEATHERING JOINT

With the design of the flexible feathering joint, our aim is to add another degree of freedom to the fin motion without additional actuators, to facilitate thrust generation with simple control for the fins. As shown in Fig. 1, there are typically three modes for the pectoral fin motion, rowing, feathering, and flapping. The rowing motion is well suited for enabling swimming and maneuvering in the horizontal plane, and is thus adopted as the pectoral fin-actuation mode for the robotic fish in this work. If the joint connecting the fin and the servo arm is rigid, the servo will have to be actuated faster during the power stroke than during the recovery stroke to produce a net thrust. However, as we show later in this paper, the body drag during the long recovery stroke will decelerate the robot and result in an overall low thrust. The proposed flexible joint design will address this problem by allowing the fin to feather passively under the drag during the recovery stroke, as shown in Fig. 2. During the power stroke, the pectoral fin will maintain the rowing motion prescribed by the servo

FIGURE 1: TYPES OF PECTORAL FIN MOTION (ADAPTED FROM [24]). THE ROTATION AXES FOR THE ROWING, FEATHERING, AND FLAPPING MOTIONS ARE VERTICAL, TRANSVERSE, AND LONGITUDINAL, RESPECTIVELY.

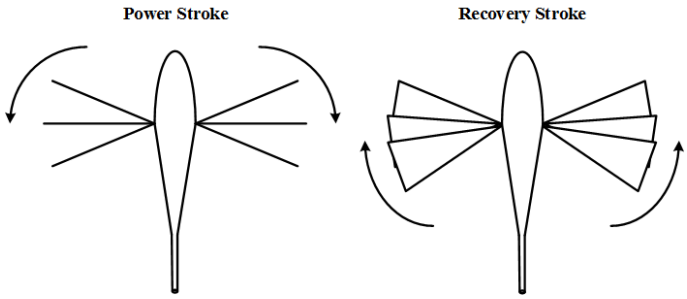

FIGURE 2: POWER AND RECOVERY STROKE SCHEMATIC OF THE PECTORAL FIN WITH FLEXIBLE FEATHERING JOINT (TOP VIEW).

to produce the maximum thrust; during the recovery stroke, the pectoral fin will feather (rotate along the transverse axis) to reduce the hydrodynamic drag on the fin, thus reducing the overall drag to the robot. Such a scheme will allow the servo to be actuated symmetrically during the power and recovery strokes, which not only simplifies the control program, but also faciliates higher robot speed with the shortened recovery stroke duration.

Fig. 3 shows the design of the proposed fin joint, which is a flexible segment connecting the servo arm to a fin-mounting structure. The latter has a slit that can accommodate fins of different sizes and materials. A stopper mechanism ensures the joint can only bend in one way. This flexible passive joint is designed with SolidWorks software and 3D-printed using a multi-material 3D printer (Connex 350 from Objet), which allows seamless integration of the flexible and rigid components in the joint. The material VeroWhite Plus (RGD835) is used for the rigid structure. Three joints with different materials and lengths for the flexible part are printed. Here the joint length refers to the length of the gap between the top and bottom rigid elements on the opposite side of the mechanical stopper. Note that the gap between the top and bottom rigid elements is almost zero on the stopper side. Length and material information for the joints are shown in Table 1. Fig. 4 shows a flexible joint mounted on a robotic fish,

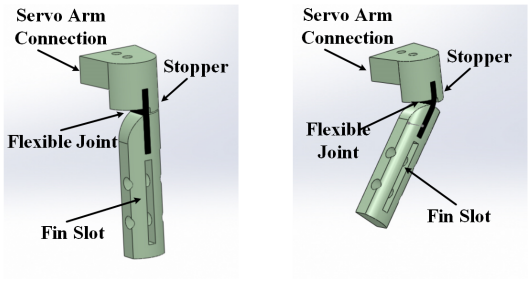

FIGURE 3: THE SCHEMATIC OF THE PROPOSED FLEXIBLE PASSIVE FEATHERING JOINT: (A) POWER STROKE, IN WHICH THE STOPPER PREVENTS FIN FROM ROTATING; (B) RECOVERY STROKE, IN WHICH THE PECTORAL FIN ROTATES AND TENDS TO ALIGN WITH THE HORIZONTAL SURFACE.

TABLE 1: SPECIFICATIONS OF THE THREE JOINTS

Joint	Length (mm)	Flexible Material
1	1	DM9850
2	1.5	DM9850
3	1.5	FLX980 (more flexible)

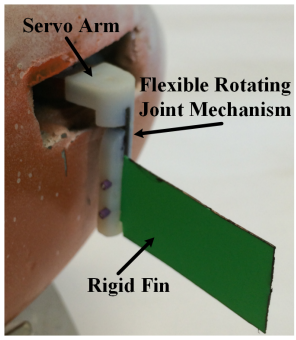

FIGURE 4: 3D-PRINTED PROTOTYPE OF THE PASSIVE JOINT.

where a rigid pectoral fin is attached to the joint.

DYNAMIC MODELING

Dynamic Model for the Robotic Fish

The robotic fish body is considered to be rigid and neutrally buoyant, surrounded by incompressible, inviscid fluid. As previously described in [18], an inertial coordinate system $[X,Y,Z]$ and a body-fixed coordinate system $[x,y,z]$ are used to model the robotic fish body motion, illustrated in Fig. 5.

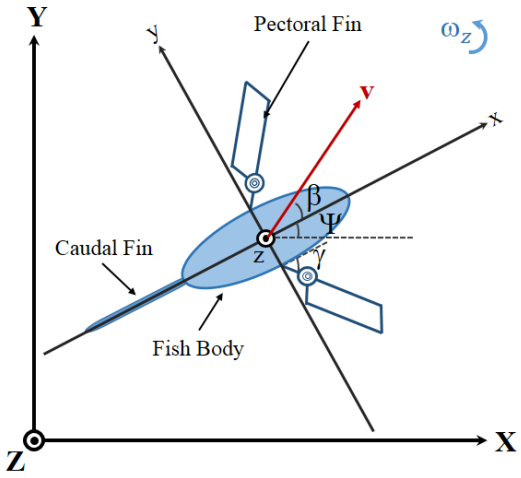

FIGURE 5: ROBOTIC FISH BODY IN PLANAR MOTION.

Since we focus on the planar motion of the robotic fish, the system will have three degrees of freedom, surge, sway, and yaw. The rigid body dynamics in the body-fixed coordinates are

$$(m_b - m_{a_x})\dot{u} = (m_b - m_{a_y})vr + f_x, \tag{1}$$
$$(m_b - m_{a_y})\dot{v} = -(m_b - m_{a_x})ur + f_y, \tag{2}$$
$$(I_z - I_{a_z})\dot{\omega} = \tau_z, \tag{3}$$

where u, v and ω are surge, sway and yaw velocities, respectively, m_b is the mass of the body, and I_z is the body inertia along the z direction. m_{a_x} and m_{a_y} are the hydrodynamic added masses of the robotic fish body along the x and y directions, respectively, and I_{a_z} is the added inertia about the z direction. f_x, f_y, and τ_z are the total force and moment exerted on the robotic fish body, which include hydrodynamic forces from the pectoral fins (see below), and the drag and lift forces and moment on the robotic fish body [18], which is described later.

The kinematics of the robotic fish body in the inertial coordinate system is represented as

$$\dot{X} = u\cos\psi - v\sin\psi, \tag{4}$$
$$\dot{Y} = v\cos\psi + u\sin\psi, \tag{5}$$
$$\dot{\psi} = \omega. \tag{6}$$

where ψ is the angle between the body-fixed and inertial coordinates, which is known as heading angle.

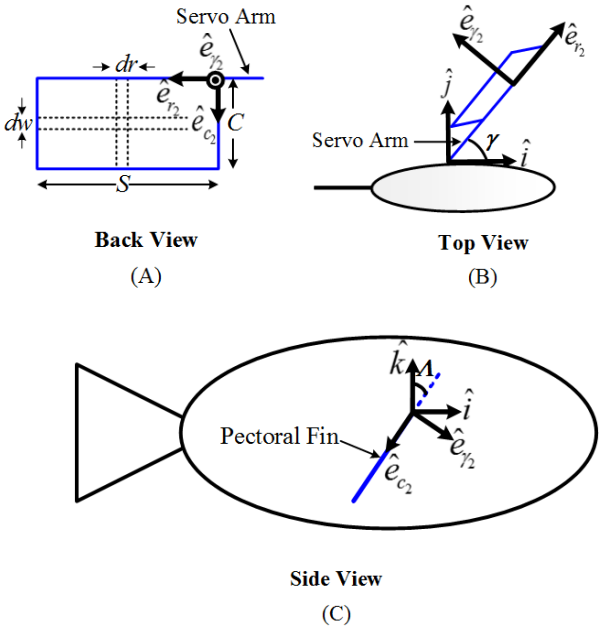

FIGURE 6: PECTORAL FIN COORDINATE SYSTEM: (A) BACK VIEW OF A RECTANGULAR PECTORAL FIN; (B) TOP VIEW OF THE ROBOTIC FISH SHOWING ONE PECTORAL FIN; (C) SIDE VIEW OF THE ROBOTIC FISH, WHERE Λ SHOWS THE FEATHERING ANGLE.

Dynamic Modeling of the Passive Feathering Joint

To be able to analyze and optimize the flexible feathering joint, one needs to understand the dynamic behavior of this joint. The first step is to model the passive joint and calculate the feathering angle Λ. Since the fin undergoes both rowing and feathering motions, hydrodynamic forces acting on the fin need to be captured in all three dimensions. We introduce a fin-fixed coordinate system and use it as a reference to model the pectoral fin, as shown in Fig. 6. The coordinate system consists of three orthonormal axes, $\{\hat{e}_{r_2}, \hat{e}_{c_2}, \hat{e}_{\gamma_2}\}$. Each pectoral fin is considered to be rigid and rectangular. The axes $\hat{e}_{r_2}$ and $\hat{e}_{c_2}$ are defined to be along the span and chord (depth) directions of the fin, respectively, while $\hat{e}_{\gamma_2}$ is perpendicular to the fin plane. Here $\{\hat{i}, \hat{j}, \hat{k}\}$ is the orthonormal basis corresponding to the body-fixed coordinates $[x, y, z]$ (Fig. 5), γ is the prescribed angle made by the servo arm with respect to the body heading $\hat{i}$ (see Fig. 5 and Fig. 6(B)), and Λ is the feathering angle (Fig. 6(C)). The relation between the fin-fixed coordinates and the body-fixed coordinates is calculated as

$$\hat{e}_{r_2} = \cos\gamma\hat{i} + \sin\gamma\hat{j} + 0\hat{k}, \tag{7}$$

$$\hat{e}_{c_2} = \sin\gamma\sin\Lambda\hat{i} - \cos\gamma\sin\Lambda\hat{j} - \cos\Lambda\hat{k}, \tag{8}$$

$$\hat{e}_{\gamma_2} = -\sin\gamma\cos\Lambda\hat{i} + \cos\gamma\cos\Lambda\hat{j} - \sin\Lambda\hat{k}. \tag{9}$$

The blade element theory [24] is used to evaluate the hydrodynamic forces on the pectoral fin. The hydrodynamic drag force produced by each element $drdw$ is evaluated as

$$d\vec{F}_{hd} = -\frac{1}{2}C_n\rho\vec{v}^2(r,w)\hat{e}_{\vec{v}}\ dwdr, \tag{10}$$

where C_n is the force coefficient, ρ is the water density, $\vec{v}(r,w)$ is the velocity of the element $drdw$, calculated in Eq. (11), and $\hat{e}_{\vec{v}}$ is a unit vector in the direction of $\vec{v}(r,w)$. The expression for $\vec{v}(r,w)$ is

$$\begin{aligned}\vec{v}(r,w) =& (r\cos\gamma + w\sin\gamma\sin\Lambda)\hat{i} + (r\sin\gamma - w\cos\gamma\sin\Lambda)\hat{j} \\ & - w\cos\Lambda\hat{k},\end{aligned} \tag{11}$$

The total hydrodynamic force is evaluated by integrating the force over the surface of the pectoral fin

$$\vec{F}_{hd} = \int_0^S\int_0^C d\vec{F}_{hd}, \tag{12}$$

where S is the span length and C is the chord length (depth) of the fin.

We model the flexible part of the joint as a pair of torsional spring and damper, connecting the pectoral fin, considered as a rigid plate, to the serve arm. Since we need to find the feathering angle Λ of the fin, the projection of the hydrodynamic force $\vec{F}_{hd}$ in $\hat{e}_{\gamma_2}$ direction produces the corresponding moment. So the moment produced by the hydrodynamic force of the pectoral fin relative to its pivot point is evaluated as

$$\vec{M}_{hd_2} = \int_0^S\int_0^C w\hat{e}_{c_2} \times dF_{hd}\hat{e}_{\gamma_2}. \tag{13}$$

The moment produced by the spring and damper at the flexible joint is evaluated as

$$\vec{M}_{(S+D)} = [-K_S\Lambda - K_D\dot{\Lambda}]\hat{e}_{r_2}, \tag{14}$$

where K_S and K_D are the spring and damping coefficients used to model the flexible passive joint.

The total moment equation of the rigid fin relative to its pivot point is written as

$$\vec{M}_{hd_2} + \vec{M}_{(S+D)} = I_{p_2}\ddot{\Lambda}, \tag{15}$$

where I_{p_2} is the effective inertia of the rigid fin. With Eq. (10), (12), and (15), the dynamics of the pectoral fin with flexible feathering joint is fully described.

The total force on the fin can be represented as

$$\vec{F}_2 = \vec{F}_{hd} + \vec{F}_{A_1} = m_{p_2}\vec{a}_2, \tag{16}$$

where $\vec{F}_{A_1}$ represents the force applied by the servo arm (through the joint) on the fin, m_{p_2} is the effective mass (fin mass and added mass) of the rigid fin, and $\vec{a}_2$ represents the acceleration of the center of mass of the fin. Similarly the total force on the servo arm can be calculated, and therefore the total force excerted on the robot body is

$$\vec{F}_{h_b} = m_{p_1}\vec{a}_1 - \vec{F}_{A_1} - \vec{F}_{hd_1}, \tag{17}$$

m_{p_1} is the effective mass of the servo arm, $\vec{a}_1$ represents the acceleration of the center of mass of the arm, and $\vec{F}_{hd_1}$ representes the hydrodynamic force of the servo arm.

The moment applied by the fin on the body is represented as

$$\vec{M}_{h_b} = \vec{r}_{cp} \times \vec{F}_{h_b}, \tag{18}$$

where $\vec{r}_{cp}$ is the vector from the the robot center of mass to the base of servo arm.

Drag and Lift on the Body

The robotic fish experiences drag and lift on its body as well as the hydrodynamic forces from the pectoral fins. The drag force F_D, lift force F_L , and the drag moment M_D acting on the robotic fish body can be represented as

$$F_D = \frac{1}{2}\rho|V_C|^2 S_A C_D, \tag{19}$$

$$F_L = \frac{1}{2}\rho|V_C|^2 S_A C_L \beta, \tag{20}$$

$$M_D = -C_M \omega_z^2 \,\mathrm{sgn}(\omega_z), \tag{21}$$

where V_C is the linear velocity of the body, S_A is the wetted area of the robot, C_D is the drag force coefficient, C_L is the lift force coefficient, C_M is the drag moment coefficient, β is the angle of attack of the fish body, ω is the angular velocity of the body along z, and sgn is the signum function.

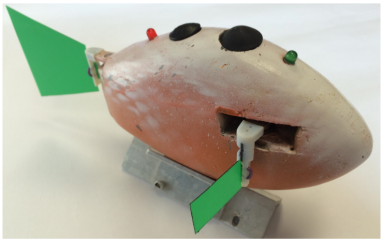

FIGURE 7: THE ROBOTIC FISH PROTOTYPE USED FOR MODEL VALIDATION. THE BODY IS DESIGNED WITH SOLIDWORKS SOFTWARE AND IS PRINTED WITH A MULTI-MATERIAL 3D PRINTER.

Finally, by adding the hydrodynamic forces and moments from the pectoral fins (Eq. (17), and (18)) and the drag and lift forces directly on the body, the terms f_x, f_y and τ_z in Eq. (1), (2), (3) can be evaluated as

$$f_x = F_{h_{b_x}} - F_D \cos\beta + F_L \sin\beta, \tag{22}$$

$$f_y = F_{h_{b_y}} - F_D \sin\beta - F_L \cos\beta, \tag{23}$$

$$\tau_z = M_{h_b} + M_D, \tag{24}$$

where $F_{h_{b_x}}$ and $F_{h_{b_y}}$ are the total hydrodynamic forces generated by pectoral fins in x and y directions.

EXPERIMENTAL RESULTS

Robotic Fish Prototype

To evaluate the presented design and dynamic model, experiments are conducted on a robotic fish prototype, which is shown in Fig. 7. The body is designed in SolidWorks software and printed utilizing the multi-material 3D printer. The printed body is 15 cm long, 8 cm high and 4.6 cm wide without the fins. The pectoral fins have 1.7 cm chord length (depth) and 3.2 cm span length. The prototype contains three Traxxas 2065 waterproof servos to actuate the pectoral fins and the caudal fin; however, the actuation of the caudal fin is not included in this study. The robotic fish also utilizes a Li-ion battery, a power converter PCB and an Arduino pro mini microcontroller board. The parameters used in the simulation are summerized in Table 2. Spring and damper coefficients of each joint are found empirically by fitting the forward swimming velocity of the robotic fish at two frequencies (0.75 Hz and 1.75 Hz), and then kept constant throughout the rest of the simulations. The fitted data for these coefficients are shown in Table 3. The experiments are conducted in a $2 \times 6 \times 2$ feet ($W \times L \times D$) tank. The forward swimming velocity is measured by a stopwatch for a 50 cm distance.

TABLE 2: IDENTIFIED PARAMETER VALUES.

Parameter	Value	unit
Added mass along x direction (m_{a_x})	1.007	Kg
Added mass along y direction (m_{a_y})	0.479	Kg
Added inertia along z direction (I_{a_z})	0.0052	Kg/m^2
Wet surface area	0.0319	m^2
Drag force coef. (C_D)	0.2131	–
Lift force coef. (C_L)	4.95	–
Drag moment coef. (C_M)	11.29×10^{-4}	Kg.m^2
Pectoral fin drag coef. (C_n)	0.4	–
Water density (ρ)	1000	Kg.m^3

TABLE 3: TORSION SPRING AND DAMPER COEFFICIENTS FOR DIFFERENT JOINTS.

Joint	K_S(N.m)	K_D(N.m.s)
1	9.36×10^{-6}	3.2×10^{-7}
2	6.24×10^{-6}	2.13×10^{-7}
3	3.41×10^{-6}	8.2×10^{-8}

Dynamic Model Validation

To validate the proposed dynamic model, two sets of experiments are conducted on the robotic fish. In the first set of experiments, the robot body is kept fixed and the feathering angle is measured. To do so, we fix the robot body by a bracket while actuating the the pectoral fins. A Casio Exilim EX-FH25 high-speed camera is used to capture the pectoral fin motion. Fig. 8 and 9 compare the measured peak values of the feathering angle and the simulation results at different fin flapping frequencies. These results are for the case where Joint 1 is used. It can be seen that the model is able to predict the feathering angle well until 2 Hz. For the two frequencies higher than 2 Hz, the discrepancy between the experimental measurement and model prediction starts to grow. This can be attributed to the constraint of the fabricated prototype, which imposes a limit on largest bending angle of the joint.

Another set of experiments are conducted when the robot is free-swimming. In these experiments, we measure the forward swimming velocity of the robotic fish using all three joints described in Table 1 and compare the results with the model predictions, shown in Fig. 10. From the figure, it can be seen that the robotic fish is able to produce effective thrust and forward swimming under symmetric actuation during power and recovery strokes. For all three joints, the predicted speeds match the experimental results well. In addition, the influence of the joint length and material is observed. Note that Joint 2 and Joint 3 have the same length, but different stiffness, while Joint 1 and Joint 2 are

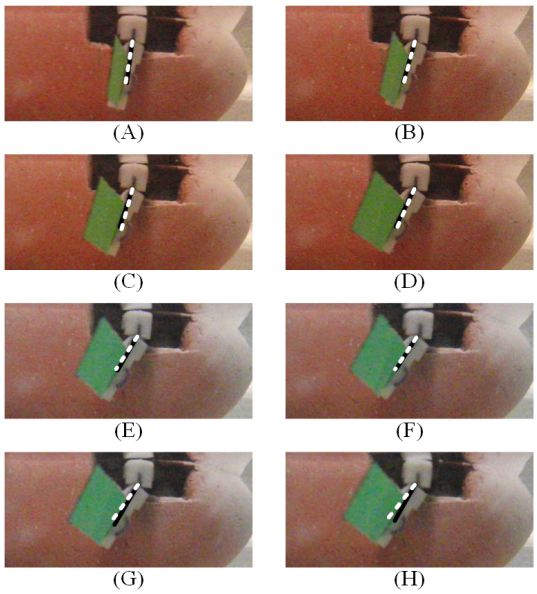

FIGURE 8: COMPARISON BETWEEN EXPERIMENTAL MEASUREMENT OF THE FEATHERING ANGLE Λ (BLACK SOLID LINE) WITH MODEL PREDICTION (WHITE DASHED LINE) OF JOINT 1, WITH FIN BEAT FREQUENCIES OF (A) 0.75 Hz, (B) 1 HZ, (C) 1.25 HZ, (D) 1.5 HZ, (E) 1.75 HZ, (F) 2HZ, (G) 2.25 HZ, AND (H) 2.5 HZ.

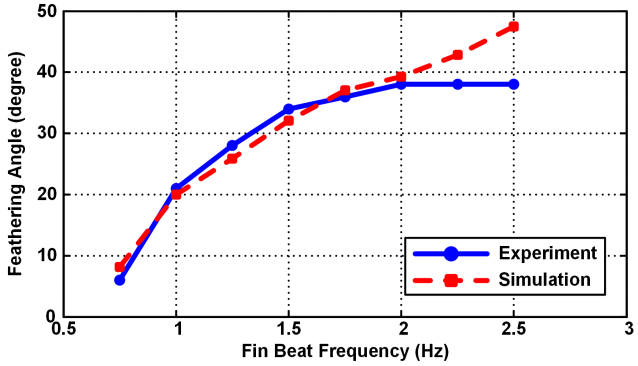

FIGURE 9: EXPERIMENTAL AND PREDICTED MEASUREMENTS OF THE FEATHERING ANGLE Λ AT EACH FREQUENCY.

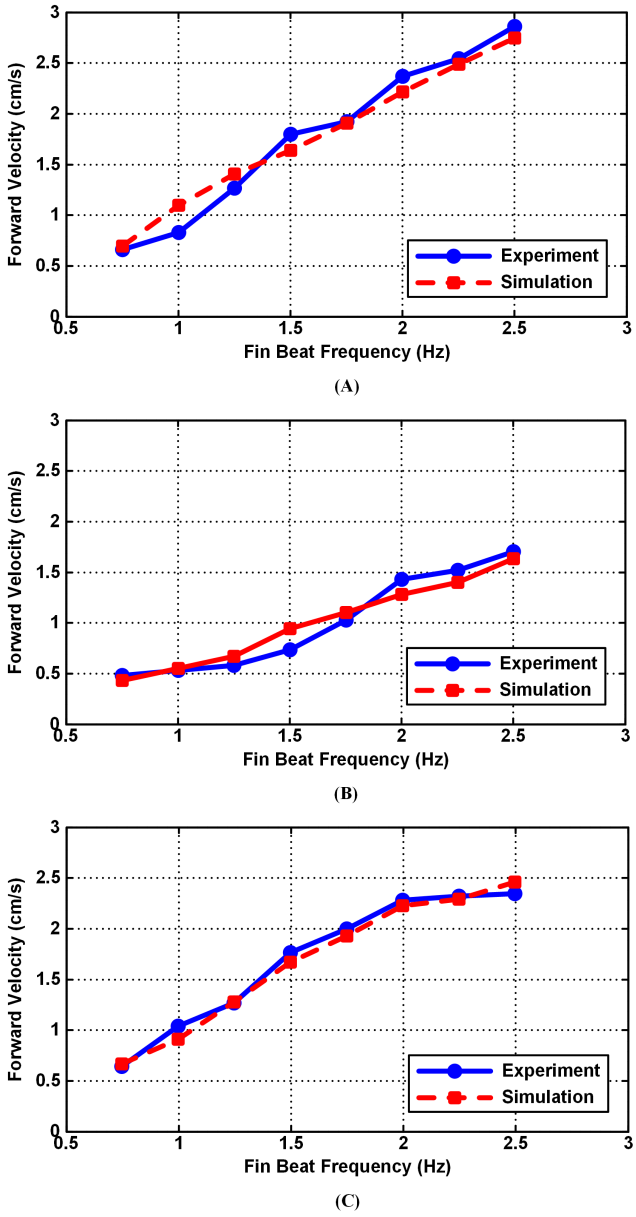

FIGURE 10: COMPARISON BETWEEN EXPERIMENTAL MEASUREMENT OF THE FORWARD SWIMMING VELOCITY WITH MODEL PREDICTION: (A) JOINT 1, (B) JOINT 2, AND (C) JOINT 3.

of the same material but with different lengths. Overall, among these three joints, the shorter and stiffer Joint 1 demonstrates the best performance. On the other hand, a stiffer and shorter joint would lead to lower maximum feathering angle. Optimization of the joint design thus presents an interesting challenge.

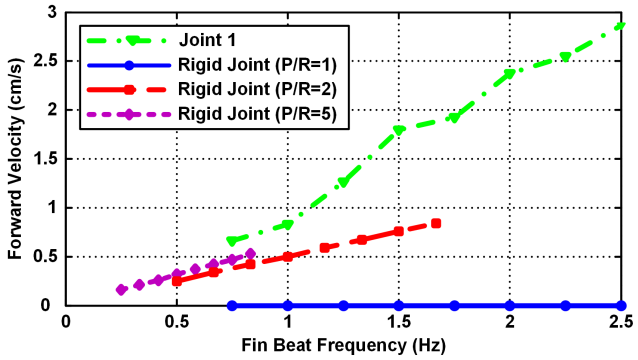

FIGURE 11: EXPERIMENTAL RESULTS FOR THE COMPARISON OF THE FORWARD SWIMMING VELOCITY VERSUS FIN BEAT FREQUENCY, FOR RIGID AND FLEXIBLE ROTATING PASSIVE JOINT.

Comparison Between the Passive Feathering Joint and the Rigid Joint

We have further compared the flexible feathering joint with the rigid joint case. This will provide a better understanding of how effective the new joint design is. In the rigid joint case, a pectoral fin is connected to the servo arm through a rigid connection, similar to the joint used in [18]. In this case, in order for the robotic fish to swim forward, we need to have different speeds for the power stroke and the recovery stroke (otherwise the net thrust would be zero) as $\frac{P}{R}$. We present the results for three cases, where $\frac{P}{R} = 1, 2$ and 5. The forward-swimming velocity for the case of using a flexible passive joint (Joint 1) is provided as well, as shown in Fig. 11. For the rigid joint case, if the total period of each fin beat cycle is T, then the overall fin beat frequency is $\frac{1}{T}$, which is what is used in Fig. 11. For all the experiments, we have run the servos up to their maximum allowed speed, which is 300°/s for Traxxas 2065. This maximum speed corresponds to the rightmost point of each curve in Fig. 11. From the figure, the speed performance of the flexible joint significantly outperforms the rigid joint cases, which affirms the effectiveness of the proposed flexible feathering joint.

CONCLUSION AND FUTURE WORK

In this study, we have proposed a novel design for a robotic fish pectoral fin joint, which enables the fin to feather in the recovery stroke while maintaining the rowing motion prescribed by the servo arm in the power stroke. This design result in 3D motion of the pectoral fin and effective thrust generation. A dynamic model for the mentioned joint is developed. To validate the proposed dynamic model, we have compared model prediction and experimental results by conducting two sets of experiments on the robotic fish incorporating the proposed joint design. The first set of experiments involve the measurement of feath-

ering angles of the fin when the robotic fish body is anchored, while the second set of experiments involve the measurement of forward speeds during free swimming of the robot. We have further confirmed the effectiveness of the joint design by comparing the swimming performance of the robot when using the proposed joint and the typical rigid joint, respectively.

The current work can be extended in several directions: First, we will use the presented dynamic model for the fin joint, along with experimental validation, to investigate the optimization of the joint design. Second, we will perform comparison of the proposed flexible feathering joint with our earlier work on flexible rowing joint [30] and potentially use the gained insight to design new joints that incorporate the strengths of both. Finally, while the results presented in this paper are based on a rigid, rectangular fin, it is of interest to extend this work to flexible pectoral fins with more general shapes.

ACKNOWLEDGMENT

The authors would like to thank John Thon and Cody Thon for their contribution in assembling the robotic fish prototype.

REFERENCES

[1] N. F. Lepora, P. l Verschure, and T. J. Prescott, "The state of the art in biomimetics," *Biomimetic and Biohybrid Systems, Lecture Notes in Computer Science, Springer*, vol. 7375, pp. 367–368, 2012.

[2] C. C. Lindsey, *Fish Phisiology-Locomotion*. Academic Press, 1978, vol. 7.

[3] J. E. Colgate and K. M. Lynch, "Mechanics and control of swimming: A review," *IEEE J. Ocean. Eng.*, vol. 29, pp. 660–673, July 2004.

[4] M. S. Triantafyllou and G. S. Triantafyllou, "An efficient swimming machine," *Scientific America*, vol. 273, no. 3, pp. 64–70, 1995.

[5] X. Deng and S. Avadhanula, "Biomimetic micro underwater vehicle with oscillating fin propulsion: System design and force measurement," in *Proc. IEEE International Conference on Robotics and Automation ICRA*, Barcelona, Spain, April 2005, pp. 3312–3317.

[6] K. A. Morgansen, T. M. L. Fond, and J. X. Zhang, "Agile maneuvering for fin-actuated underwater vehicles," in *Proc. 2006 2nd Int. Symp. Commun., Control Signal Process.*, 2006.

[7] P. Kodati and X. Deng, "Experimental studies on the hydrodynamics of a robotic ostraciiform tail fin," in *Proceedings of IEEE / RSJ International Conference on Intelligent Robots and Systems*, Beijing, China, October 2006, pp. 5418–5423.

[8] M. Aureli, V. Kopman, and M. profiri, "Free locomotion of underwater vehicles actuated by ionic polymer metal composites," in *IEEE / ASME Transactions on Mechatronics*, August 2010, pp. 603–614.

[9] S. Guo, T. Fukuda, and K. Asaka, "A new type of fish-like underwater microrobot," *IEEE/ASME Transactions on Mechatronics*, vol. 8, no. 1, pp. 136–141, 2003.

[10] K. H. Low, "Locomotion and depth control of robotic fish with modular undulating fins," *International Journal of Automation and Computing*, vol. 4, pp. 348–357, 2006.

[11] X. Tan, D. Kim, N. Usher, D. Laboy, J. Jackson, A. Kapetanovic, J. Rapai, B. Sabadus, and X. Zhou, "An autonomous robotic fish for mobile sensing," in *Proc. IEEE / RSJ International Conference on Intelligent Robots and Systems*, Beijing, China, October 2006, pp. 5424–5429.

[12] X. Tan, "Autonomous robotic fish as mobile sensor platforms: Challenges and potential solutions," *Marine Technology Society Journal*, vol. 45, no. 4, pp. 31–40, July 2011.

[13] F. Zhang, J. Thon, C. Thon, and X. Tan, "Miniature underwater glider: Design, modeling, and experimental results," in *Proc.IEEE International Conference on Robotics and Automation*, St. Paul, MN, May 2012, pp. 4904–4910.

[14] S. Marras and M. Porri, "Fish and robots swimming together: Attraction towards the robot demands biomimetic locomotion," *Journal of the Royal Society Interface*, vol. 9, no. 73, pp. 1856–1868, August 2012.

[15] K. A. Morgansen, B. I. Triplett, and D. J. Klein, "Geometric methods for modeling and control of free-swimming fin-actuated underwater vehicles," *IEEE Transaction on Robotics*, vol. 23, no. 6, pp. 1184–1199, December 2007.

[16] J. Wang, P. K. McKinley, and X. Tan, "Dynamic modeling of robotic fish with a flexible caudal fin," in *Proceedings of the ASME 2012 5th Annual Dynamic Systems and Control Conference joint with the JSME 2012 11th Motion and Vibration Conference, Paper DSCC2012-MOVIC2012-8695*, Ft. Lauderdale, Florida, 2012.

[17] J. Wang and X. Tan, "A dynamic model for tail-actuated robotic fish with drag coefficient adaptation," *Mechatronics*, vol. 23, no. 6, pp. 659–668, 2013.

[18] S. B. Behbahani, J. Wang, and X. Tan, "A dynamic model for robotic fish with fexible pectoral fins," in *Proceedings of 2013 IEEE/ASME International Conference on Advanced Intelligent Mechatronics*, Wollongong, Australia, 2013, pp. 1552–1557.

[19] G. V. Lauder, P. G. A. Madden, R. Mittal, H. Dong, and M. Bozkurttas, "Locomotion with flexible propulsors: I. experimental analysis of pectoral fin swimming in sunfish," *Bioinsp. Biomim.*, vol. 1, pp. S25–S34, 2006.

[20] R. Mittal, H. Dong, M. Bozkurttas, G. V. Lauder, and P. Madden, "Locomotion with flexible propulsors: Ii. computational modeling of pectoral fin swimming in sunfish," *Bioinsp. Biomim.*, vol. 1, pp. S35–S41, 2006.

[21] J. Palmisano, R. Ramamurti, K. J. Lu, J. Cohen, W. Sandberg, and B. Ratna, "Design of a biomimetic controlled-

curvature robotic pectoral fin," in *IEEE International Conference on Robotics and Automation*, Rome, Italy, April 2007, pp. 966–973.

[22] J. A. Walker, "Dynamics of pectoral fin rowing in a fish with an extreme rowing stroke: The threespine stickleback (gasterosteus aculeatus)," *Journal of Experimental Biology*, vol. 207, pp. 1925–1939, May 2004.

[23] P. W. Webb, *Hydrodynamics and Energetics of Fish Propulsion*. Department of the Environment Fisheries and Marine Service, 1975.

[24] R. W. Blake, *Fish Locomotion*. Cambrige: Cambrige University Press, 1983.

[25] P. Kodati, J. Hinkle, A. Winn, and X. Deng, "Microautonomous robotic ostraciiform (macro): Hydrodynamics, design and fabrication," *IEEE Transaction on Robotics*, vol. 24, pp. 105–117, February 2008.

[26] N. Kato, "Guidance and control of fish robot with apparatus of pectoral fin motion," in *Proc. IEEE International Conference on Robotics and Automation*, Leuven, Belgium, May 1998, pp. 446–451.

[27] N. Kato and M. Furushima, "Pectoral fin model for maneuver of underwater vehicle," in *Proc. Symposium on Autonomous Underwater Vehicle Technology*, June 1996, pp. 49–56.

[28] D. Lachat, A. Crespi, and A. J. Ijspeert, "Boxybot: A swimming and crawling fish robot controlled by a central pattern generator," in *Proc. 1st IEEE / RAS-EMBS Int. Conf. Biomed. Robot. Biomechatron. BioRob 2006*, February 2006, pp. 643–648.

[29] J. L. Tangorra, N. Davidson, I. W. Haunter, P. G. A. Madden, and G. V. Lauder, "The development of a biologically inspired propulsor for unmanned underwater vehicles," vol. 23, no. 3, pp. 533–550, July 2007.

[30] S. B. Behbahani and X. Tan, "A fexible passive joint for robotic fish pectoral fins: Design, dynamic modeling, and experimental results," in *Proceedings of the 2014 IEEE/RSJ International Conference on Intelligent Robots and Systems*, Chicago, IL, 2014, p. under review.